analytical chemistry

Article

Cite This: Anal. Chem. 2017, 89, 11664-11671

pubs.acs.org/ac

Metabolomics of Small Numbers of Cells: Metabolomic Profiling of 100, 1000, and 10000 Human Breast Cancer Cells

Xian Luo and Liang Li*

Department of Chemistry, University of Alberta, Edmonton, Alberta T6G 2G2, Canada

Supporting Information

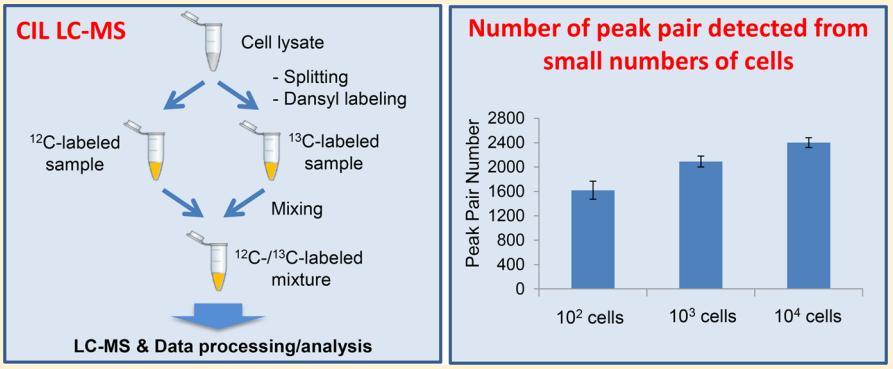

ABSTRACT: In cellular metabolomics, it is desirable to carry out metabolomic profiling using a small number of cells in order to save time and cost. In some applications (e.g., working with circulating tumor cells in blood), only a limited number of cells are available for analysis. In this report, we describe a method based on high-performance chemical isotope labeling (CIL) nanoflow liquid chromatography mass spectrometry (nanoLC-MS) for high-coverage metabolomic analysis of small numbers of cells (i.e., ≤10000 cells). As an example, ^{12}C-/^{13}C-dansyl labeling of the metabolites in lysates of 100, 1000, and 10000 MCF-7 breast cancer cells was carried out using a new labeling protocol tailored to handle small amounts of metabolites. Chemical-vapor-assisted ionization in a captivespray interface was optimized for improving metabolite ionization and increasing robustness of nanoLC-MS. Compared to microflow LC-MS, the nanoflow system provided much improved metabolite detectability with a significantly reduced sample amount required for analysis. Experimental duplicate analyses of biological triplicates resulted in the detection of 1620 ± 148, 2091 ± 89 and 2402 ± 80 (n = 6) peak pairs or metabolites in the amine/phenol submetabolome from the ^{12}C-/^{13}C-dansyl labeled lysates of 100, 1000, and 10000 cells, respectively. About 63−69% of these peak pairs could be either identified using dansyl labeled standard library or mass-matched to chemical structures in human metabolome databases. We envisage the routine applications of this method for high-coverage quantitative cellular metabolomics using a starting material of 10000 cells. Even for analyzing 100 or 1000 cells, although the metabolomic coverage is reduced from the maximal coverage, this method can still detect thousands of metabolites, allowing the analysis of a large fraction of the metabolome and focused analysis of the detectable metabolites.

Cellular metabolomics involves the study of metabolomic profiles and their associated changes in response to a stimuli or perturbation to a cell (e.g., exposure to a toxin or mutation of a gene). It can be a powerful tool for studying cell biology and looking for potential biomarkers of diseases. In order to increase the number of quantifiable metabolites in a cell extract, multiple analytical techniques, with each often run under several different experimental conditions, are employed,[1,2] which requires the use of a large number of cells (e.g., millions of cancer cells). However, decreasing the number of cells required for metabolomics would significantly benefit a number of research areas. For biological studies, with a reduced cell number required, one does not need to culture many cells, thereby reducing the overall experimental cost and allowing more biological replicates to be conveniently performed (e.g., no need of pooling cell cultures). In other areas, such as researches on stem cells,[3] circulating tumor cells in blood,[4] and primary cells from tissues procured using laser capture microdissection (LCM),[5] only a limited number of cells are available.

Analysis of metabolites from small numbers of cells, or even single cell, has been attempted by a number of detection techniques including electrochemical detection, vibrational spectrometry, fluorescence-based detection, and mass spectrometry (MS).[6,7] Among them, only MS has the potential to analyze many metabolites simultaneously with high specificity. For example, matrix-assisted laser desorption ionization (MALDI) can generate ions from a small sample spot, offering the possibility of detecting cellular components from a few

Received: August 2, 2017
Accepted: October 13, 2017
Published: October 13, 2017

DOI: 10.1021/acs.analchem.7b03100
Anal. Chem. 2017, 89, 11664−11671

cells[8] or even a single small-size cell (e.g., hemoglobin from a red blood cell[9] and metabolites from HeLa cells[10]). However, low MALDI efficiency of metabolites and strong interference of matrix ions in low mass region can limit the number of detectable metabolites. Matrix-free laser desorption ionization from a sample placed onto an active desorption substrate may eliminate matrix interference, but achieving uniformly high ionization efficiency for many metabolites is still a challenge. Some studies have shown the detection of about 100 metabolites and lipids from 1 to 80 cells.[11] An alternative approach of using laser ablation electrospray ionization from a sample spot has shown the possibility of detecting 332 putative metabolite features in 13 *A. Cepa* cells.[12] Electrospray ionization (ESI) MS is another sensitive technique that has been shown to be useful to detect metabolites and lipids from a few cells or single plant cell.[13,14]

The studies noted above only provided a few examples of using MS for analyzing small numbers of cells; excellent reviews on this active research field can be found in the literature.[6,7] Currently, the major challenges are metabolomic coverage and quantification. Because lipids are major constituents of a cell and, therefore, are in high abundance, MS analysis of small numbers of cells detected more lipids than metabolites, even within the small number of mass spectral features observed. Moreover, cellular metabolomics requires accurate and precise quantification of metabolic changes among comparative cell types (i.e., relative quantification of individual metabolite concentrations among different cells). Without using internal standards, MALDI, ESI and other ionization methods suffer from matrix and ion suppression effects in metabolite quantification. Thus, there is a clear need of developing more sensitive and quantitative tools to perform high-coverage metabolomic profiling of small numbers of cells.

Recognizing that chemical derivatization can improve the sensitivity of metabolite detection in MS, a number of research groups have reported various labeling reagents and chemistries targeting the analysis of metabolites of interest with varying degrees of success.[15−25] We have been involved in developing a high-performance chemical isotope labeling (CIL) liquid chromatography mass spectrometry (LC-MS) platform for quantitative metabolomics.[26] In our previous studies, we have reported a divide-and-conquer approach of performing deep profiling of the metabolome using four labeling chemistries: ^{12}C-/^{13}C-dansyl labeling for the amine/phenol submetabolome,[26] ^{12}C-/^{13}C-DmPA labeling for the carboxylic submetabolome,[27] base-activated ^{12}C-/^{13}C-dansyl labeling for the hydroxyl submetabolome,[28] and ^{12}C-/^{13}C-dansylhydrazine labeling for the carbonyl submetabolome.[29] These four submetabolomes can cover over 95% of the entire chemical space of the endogenous metabolites in the human metabolome database.[29] These rationally designed labeling methods afford a significant increase in metabolite detectability using reversed phase (RP) LC-MS without the need of changing columns and ionization modes. In addition, using differential isotope labeling, relative quantification of individual metabolites can be carried out with high accuracy and precision.

In this report, we describe a method of performing high-coverage quantitative metabolomics from small numbers of cells using CIL nanoflow LC-MS. To analyze small numbers of cells, previous CIL LC-MS protocols, such as that reported by Luo et al. for analyzing 10^8 yeast cells,[30] cannot be adapted. Because of the need to deal with much smaller amounts of metabolites present in a few cells, compared to analyzing millions of cells, a very sensitive workflow for CIL LC-MS is required. Thus, we focused our research efforts on developing and optimizing each key step from cell lysis to data generation to minimize sample loss during the sample workup and maximize metabolite detection in MS. We also focused on the metabolome profiling of an analytically more challenging cell type: small-size mammalian cells. This type of cells is far more widely employed in biological studies and biomarker discovery, compared to other types of cells such as yeast cells or large-size cells, thus increasing the overall impact of the analytical workflow for cellular metabolomics research. In this work, we demonstrate the performance of a sensitive workflow in the analysis of 100, 1000, and 10000 MCF-7 breast cancer cells using dansylation labeling for profiling the amine/phenol submetabolome with unprecedented metabolomic coverage.

EXPERIMENTAL SECTION

Overall Workflow. Figure 1 shows the overall workflow for metabolomic profiling of a small number of cells. MCF-7 breast cancer cells, representative of many different types of mammalian cells commonly used in biological studies, were cultured, harvested, washed, counted, and then aliquoted to separate vials. Cell metabolism was quenched by snap-freezing in liquid nitrogen. The cells were lyzed using a glass-bead-assisted lysis method (see below). The cell extracts were separated from glass beads and cell debris by centrifugation, and then dried down. The extracts were redissolved in Na_2CO_3/$NaHCO_3$ buffer, aliquoted, and labeled using ^{12}C- and ^{13}C-dansylation separately. The ^{12}C- and ^{13}C-labeled samples were mixed by 1:1 (v/v), and dried down. The dried samples were redissolved in 9:1 (v/v) H_2O:ACN and analyzed by LC-MS. To improve detection sensitivity, nanoLC-MS with a Bruker captivespray ionization (CSI) interface was used. CSI uses a nontaped emitter tip which is not easily clogged, allowing

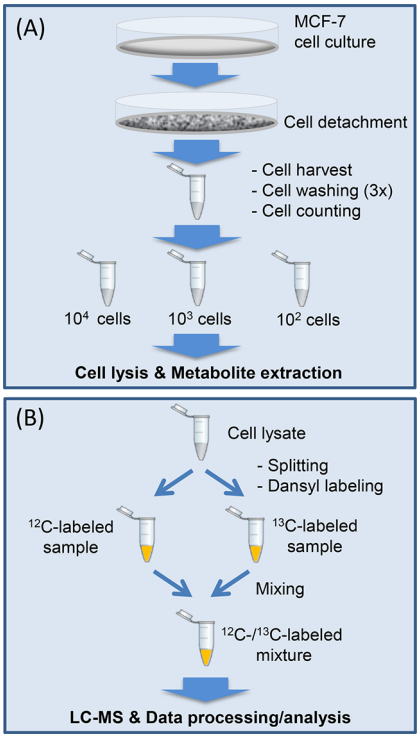

Figure 1. Workflow for CIL LC-MS method development.

DOI: 10.1021/acs.analchem.7b03100
Anal. Chem. 2017, 89, 11664−11671

robust operation in running complex (and often precious) metabolomic samples. We also employed and optimized a chemical-vapor-assisted technique to further increase MS sensitivity.

Cell Culture and Harvest. MCF-7 cells (ATCC HTB-22) were cultured in Hyclone DMEM medium, supplemented with 10% fetal bovine serum (FBS) and 0.01 mg/mL human recombinant insulin, in 10 cm diameter culture dishes at 37 °C in a humidified atmosphere with 5% CO_2. The growth medium was renewed every 2 days. For cell harvest, the cells were treated by 0.25% (w/v) trypsin and 0.53 mM EDTA at 37 °C. The trypsinization process, monitored under a Zeiss Axiovert 25 inverted microscope (Oberkochen, Germany), was inhibited by adding the growth medium when the rounded cells were in suspension. The trypsin and growth medium were removed by centrifugation at 125*g* for 5 min at 4 °C. The cell pellets were suspended in 1 mL of cold PBS solution and centrifuged at 125*g* for 5 min at 4 °C. After removing PBS, this washing procedure was repeated by two more times. The washed cells in PBS were counted by a hemocytometer, and different numbers of cells were aliquoted into separate vials. The vials were snap-frozen in liquid nitrogen and then stored at −80 °C freezer until further use.

Cell Lysis and Metabolite Extraction. Cell lysis was carried out by the glass-bead-assisted method.[30] For comparison, ultrasonication cell lysis was also examined using a Branson Sonifer 450 Ultrasonic Distrupteror (Danbury, CT). For ultrasonic lysis, the cells were suspended in 1 mL of 50% MeOH, and sonicated on ice-bath for 1 min. For glass-bead lysis, 50 μL of lysis solvent and 0.1 mL of 0.5 mm diameter glass beads (Biospec Products, Bartlesville, OK) were added into the cell vial. The vials were vortexed on a VORTEX-GENIE 2 Mixer holder for 10 min at 4 °C. Then additional 400 μL of the same lysis solvent were added and vortexed for 10 min for metabolite extraction. After centrifugation at 16000*g* for 10 min, the supernatant was transferred to another vial and dried down in Speed Vac (Savant SC110A). The lysis/extraction solvent examined included 50% (v/v) ACN in water, 50% (v/v) MeOH in water, and a combination solvent of 1:1:1 (v/v/v) ACN/MeOH/H_2O (AMW; see Results and Discussion).

Dansylation Labeling. For microflow LC-MS analysis of a large number of cells (i.e., 10^5 cells in this work), a cell extract was redissolved in 50 μL of water and labeled using a previously reported protocol.[30] In brief, a 20 μL aliquot of the extract was taken and mixed with 10 μL of Na_2CO_3/$NaHCO_3$ buffer and 10 μL of ACN. The solution was spun down and mixed with 20 μL of ^{12}C-dansyl chloride (DnsCl) solution (18 mg/mL in ACN) for light labeling. The reaction mixture was incubated at 40 °C for 1 h. After 1 h, the mixture was cooled down on ice−water bath, and 4 μL of 250 mM NaOH was added to quench the reaction by consuming the excess DnsCl. The solution was then incubated at 40 °C for another 10 min. Finally, 20 μL of 425 mM formic acid (FA) in 1:1 ACN/H_2O was added to consume excess NaOH and to acidify the solution. For heavy labeling using ^{13}C-dansyl chloride (available from mcid.chem.ualberta.ca), another 20 μL aliquot of the extract was taken and processed in the same way as ^{12}C-labeling. The ^{12}C-labeled sample was mixed with the ^{13}C-labeled sample in 1:1 (v/v) for microflow LC-MS analysis.

For analyzing small numbers of cells (≤10^4 cells), a new labeling protocol was developed to handle the small amounts of metabolites in the cell extracts. The cell extract from 100, 1000, or 10000 cells was redissolved in 20 μL of Na_2CO_3/$NaHCO_3$ buffer, and split into two aliquots for labelings. Due to the presence of precipitates in the redissolved cell extract, 7.5 μL, instead of 10 μL, was taken into a 0.6 mL vial for ^{12}C-labeling and another 7.5 μL was taken for ^{13}C-labeling. An aliquot of 7.5 μL of 0.25 mg/mL DnsCl in ACN was added to each vial and the reaction mixture was incubated at 40 °C for 1 h, and then quenched by adding 1 μL of 250 mM NaOH. An aliquot of 5 μL of 425 mM FA was added to consume the excess NaOH. The ^{12}C- and ^{13}C-labeled samples were mixed in 1:1 (v/v) and dried down in Speed Vac and redissolved in 20 μL of 9:1 (v/v) H_2O:ACN for nanoflow LC-MS analysis.

LC-UV Quantification. The total amount of labeled metabolites was determined by using a step-gradient LC-UV method.[31] The procedure used is shown in Supporting Information, Note S1.

Microflow LC-MS. For profiling the metabolites in 10^5 cells, Thermo Scientific UltiMate 3000 UHPLC (Sunnyvale, CA) connected to a Bruker Maxis II Quadrupole Time-of-flight (Q-TOF) mass spectrometer (Billerica, MA) was used. The ^{12}C-/^{13}C-labeled samples were injected into an Agilent reversed phase Eclipse Plus C18 column (2.1 mm × 10 cm, 1.8 μm particle size, 95 Å pore size) for separation. The LC-MS conditions are shown in Supporting Information, Note S1.

Nanoflow LC-MS. The analyses of cell extracts from small numbers of cells were performed on a nanoflow LC-MS system. It consisted of Waters NanoAcquity UPLC (Milford, MA) connected to a Bruker Impact HD Q-TOF mass spectrometer (Billerica, MA) equipped with a captivespray nanoBooster ion source (Bruker). Chromatographic separations were performed on a Thermo Scientific Acclaim PepMap 100 trap column (75 μm × 20 mm, 3 μm) and Acclaim PepMap RSLC C18 column (75 μm × 150 mm, 2 μm; Sunnyvale, CA). The LC-MS conditions used are shown in Supporting Information, Note S1.

Data Processing and Metabolite Identification. The raw LC-MS data were exported as CSV files by Bruker Daltonics Data Analysis 4.3. A software tool, IsoMS,[32] was used to extract the peak pairs from the CSV files, filter the peak pairs by removing redundant peaks such as adduct ions, dimers and multimers to retain only $[M + H]^+$ pairs (i.e., one peak pair corresponds to one unique metabolite), and calculate the peak-pair intensity ratios of individual labeled metabolites.[33] The multiple files generated from different LC-MS runs were aligned together by their accurate mass and retention time, and missing values in aligned files were filled by the Zerofill software.[34] Metabolite identification was done by searching against the dansyl standard library[35] and MyCompoundID (MCID) libraries (www.mycompoundid.org).[36]

RESULTS AND DISCUSSION

Cell Lysis and Metabolite Extraction. In cellular metabolomics, efficient cell lysis and metabolite extraction are very important, especially for profiling a small number of cells. In addition, the lysis method should be compatible to downstream sample processing and analysis. Detergent-based cell lysis is often used for cellular proteomics.[37] However, for metabolomics, detergent is difficult to separate from the metabolites and may cause interference in chemical labeling and LC-MS. Cell lysis by a physical means is a better option. Ultrasonic cell lysis is perhaps the most widely used method.[38] However, a lot of energy is absorbed in this process, which may cause metabolite degradation. It also has a low throughput, as only one sample can be processed each time using a

DOI: 10.1021/acs.analchem.7b03100
Anal. Chem. 2017, 89, 11664−11671

conventional ultrasonic tip. In addition, there is a risk of cross-contamination if the tip is not washed thoroughly.

Recently, we reported a workflow for yeast cell metabolomic profiling where a glass-bead-assisted method was optimized for efficient lysis of yeast cells.[30] The cells were disrupted by shear force generated from glass beads during vortexing. Comparing to ultrasonic lysis, the glass-bead method does not produce much heat, can be performed in parallel for multiple samples when a vortex holder is used, and there is no risk of cross-contamination. However, in this work, our focus was to develop a sensitive workflow for metabolomic profiling of small-size mammalian cells, which are prone to metabolite leak during harvesting and cell washing step, compared to yeast cells which have a much stronger cell membrane. Thus, it is much easier to lose metabolites during the sample workup in analyzing mammalian cells. Sample loss may not be a problem if one has a lot of cells to start with. However, when we are forced to deal with small numbers of cells, any sample loss will result in the loss of metabolome information. In order to develop a method to lyse mammalian cells efficiently, we have compared the efficiencies of the ultrasonic and glass-bead methods. Figure 2A shows the number of peak pairs detected from microflow

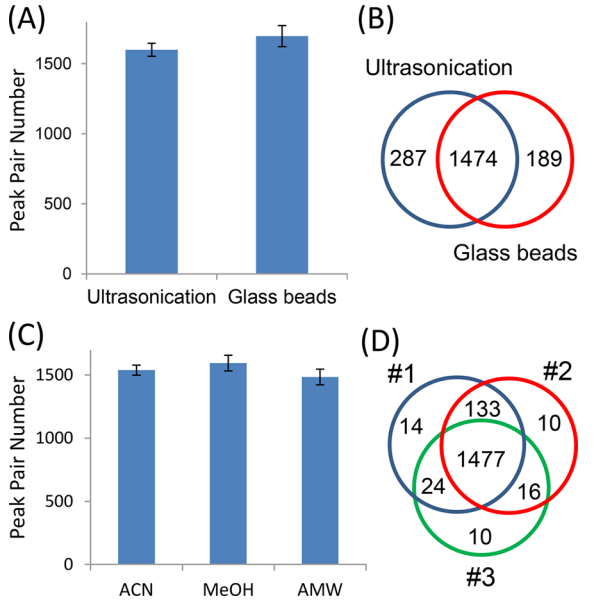

Figure 2. (A) Comparison of peak pair numbers detected from the ultrasonic cell lysis method and the glass-bead-assisted cell lysis method. (B) Venn diagram of peak pair numbers from the two methods. (C) Comparison of peak pair numbers detected from different metabolite extraction solvents. (D) Venn diagram of peak pair numbers detected from biological triplicate analysis using MeOH extraction. Data were from experimental triplicate analysis of three biological replicates (n = 9).

LC-MS analysis of ^{12}C-/^{13}C-labeled cell extracts prepared with a starting material of 10^5 cells. There were 1599 ± 47 (n = 9) peak pairs detected from ultrasonic lysis and 1697 ± 76 (n = 9) peak pairs detected from the glass-bead method. These numbers are not significantly different, although the average peak pair number per run is slightly higher in the glass-bead method. Figure 2B shows the Venn diagram of the peak pair numbers detected from the two methods; only the peak pairs commonly detected in more than half of the LC-MS runs in each method were included for comparison. Most of the peak pairs are in common (within a mass tolerance of 10 ppm), but more unique pairs are detected in the ultrasonic method, which may be related to the formation of degraded metabolites during the sonication process. Based on these comparison results, we chose the glass-bead method for lysing the MCF-7 cells.

Selection of a proper extraction solvent is also important in cellular metabolomics. Based on literature information and our own experience,[39] we selected and compared three solvent systems: 50% (v/v) ACN in water, 50% (v/v) MeOH in water, and a combination solvent of 1:1:1 (v/v/v) ACN/MeOH/H_2O (AMW). In this case, 10^5 cells were lysed with the glass-bead method and extracted using one of the three solvents, followed by dansyl labeling and microflow LC-MS analysis. As Figure 2C shows, there are 1539 ± 40, 1594 ± 62, and 1484 ± 62 (n = 9) peak pairs detected from 50% ACN, 50% MeOH, and AMW extraction, respectively. These numbers are not significantly different, although 50% MeOH extraction gives a slightly larger number. The reproducibility of extraction was found to be excellent. As an example, the Venn diagram of the peak pair numbers detected in triplicate analysis using 50% MeOH extraction (Figure 2D) shows that 1477 peak pairs (92.7%) were commonly detected in triplicates (see Supporting Information, Figure S1 for the ACN and AMW extractions). From the comparison results obtained, we selected 50% MeOH in water as the extraction solvent for the workflow.

Dansylation Protocol. The previously reported dansylation protocol was useful for analyzing samples with a total concentration of labeled metabolites of >1 mM.[26,30] We found that it was not suitable for labeling a cell extract from a small number of cells. One reason is related to the presence of high concentrations of dansyl dimethylamine and dansyl amine, two major byproducts, when using high concentrations of dansyl chloride to label low concentrations of samples. These two products are detected in LC-MS as two high-intensity chromatographic peaks that can interfere with the quantification of other coeluting labeled metabolites (e.g., signal saturation in MS detection). Another reason is related to the presence of a large amount of dansyl hydroxyl (Dns-OH), a product from the labeling quenching step, in a labeled sample. Dns-OH can suppress other labeled metabolites in nanoLC-MS analysis. In microflow LC-MS, Dns-OH can be eluted out at the first 2 min of the ion chromatogram. However, in nanoLC-MS, a trapping column is used to capture the labeled metabolites before injecting them into the analytical column for separation. After sample trapping, the relatively hydrophilic Dns-OH is washed away using a high-water-content solvent. Even with the use of an additional washing step, Dns-OH cannot be removed completely. Extension of the washing time or an increase in the number of washings is not ideal, as this will elongate the total analysis time and increase the risk of losing hydrophilic metabolites.[35]

To address the above issues, we decreased the DnsCl concentration for the labeling reaction and used a small volume of buffer to redissolve a cell lysate to keep the metabolite concentration high. We tested the method blank labeled by different concentrations (0.25, 0.5, 1 mg/mL) of DnsCl in nanoLC-MS. The signals of Dns-OH, Dns-dimethylamine, and Dns-amine were significantly reduced when a lower concentration of DnsCl was used (Supporting Information, Figure S2). Some dansyl labeled background chemicals in the labeled blanks were observed. However, when the DnsCl concentration was decreased to 0.25 mg/mL, these background peaks became very small. Moreover, using this concentration to label a real

DOI: 10.1021/acs.analchem.7b03100
Anal. Chem. 2017, 89, 11664−11671

cell lysate resulted in the detection of thousands of metabolites in nanoLC-MS (see below). Thus, in our workflow, we chose 0.25 mg/mL of DnsCl to label the cell lysates from small numbers of cells.

Captivespray MS. Metabolite detectability can be significantly affected by the MS setup and experimental conditions used. At present, most of the metabolomic analysis experiments are done using a conventional or microflow ESI-MS, while there are only a few reports of using nanoESI-MS.[40−44] The captivespray ion source employed in this work for nanoflow LC-MS uses a gas stream to guide the nanospray-generated ions into the mass spectrometer. Comparing to nanoESI, there is no need for *X*, *Y*, *Z* positioning in CSI, and the nontapered emitter spray tip avoids being easily clogged for robust operation. There is no report of using captivespray for metabolomic analysis and thus we intended to optimize the CSI setup for CIL LC-MS analysis of cell extracts from small numbers of cells.

We also applied and optimized a chemical-vapor-assisted ESI technique in CSI to improve detection sensitivity.[45] In this technique, a chemical is placed in a container and nitrogen gas flows through the container to carry the chemical vapor to the spray tip chamber. Our group previously demonstrated that this technique could enhance the MS sensitivity in shotgun proteomics, when an appropriate chemical (e.g., butanol) was used.[45] In this study, we evaluated four different dopant gas: ACN, MeOH, isopropanol (IPA), 20% FA in ACN for metabolome analysis using CIL LC-MS. The physical properties of the four chemicals can be found in Supporting Information, Table S1. Dansyl labeled cell lysates were analyzed using CSI MS under different chemical vapors, and several amino acids detected were selected to evaluate the performance. Figure 3A shows the signal comparison of labeled amino acids detected in cell lysates. Overall, the use of ACN provided the highest signal enhancement for all the analytes. Although these analytes have different chemical/physical properties, the signal enhancement had the same trend. This can be attributed to the presence of the dansyl tag(s) in each analyte that equalizes the ionization process to some extent and, as a result, different metabolites have similar behaviors in the ionization process. Based on these results, we chose pure ACN as the dopant gas for the subsequent studies. While the exact mechanism for signal enhancement by using ACN dopant is unclear, we speculate that the enhancement was due to enhanced ionization efficiencies for the dansylated metabolites during the ESI process. It is plausible that ACN vapor molecules surrounding the ESI droplets might reduce the energy barriers required for ejecting the analyte ions from the droplet surfaces to the gas phase.

Two other adjustable parameters in CSI were optimized. Figure 3B and C show the effects of dry gas (nitrogen) temperature and capillary voltage on normalized ion signals of four selected amino acids, respectively. The optimal temperature of 200 °C and capillary voltage of 1400 V were chosen.

Injection Amount. The amount of samples injected into LC-MS can also have a significant effect on metabolite detectability. Since the total concentration of labeled metabolites is measured by LC-UV in our workflow, we can readily determine the optimal injection amount that gives the maximal number of peak pairs detectable by LC-MS. Optimization of the injection amount was performed on both microflow LC-MS and nanoLC-MS for comparison. In this case, a series of different volumes of ^{12}C-/^{13}C-labeled cell

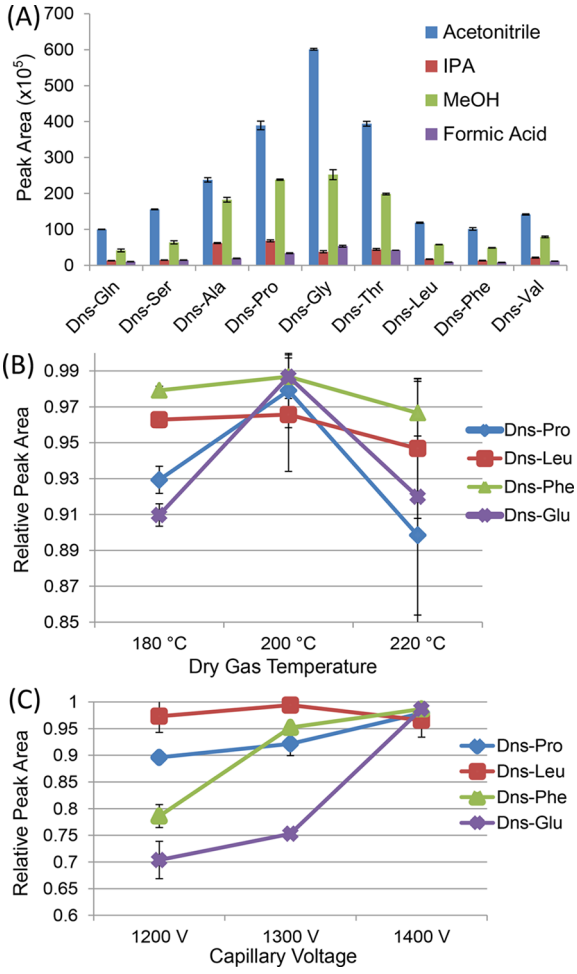

Figure 3. (A) Peak areas of molecular ions of nine dansyl labeled metabolites detected with the use of different dopant chemical vapors. Normalized peak areas of molecular ions of four dansyl labeled metabolites detected at (B) different temperatures of dry gas and (C) different capillary voltages. Data were from experimental triplicate analysis (n = 3).

lysates from 10^5 cells were injected into microflow LC-MS, while a labeled cell lysate from 10^4 cells was diluted and then injected into nanoLC-MS. Figure 4A and B show the number of peak pairs detected from two systems, respectively. In Figure 4A, as the injection amount increases, the peak pair number detected by microflow LC-MS increases and then levels off at 2.04 nmol. On average, 1680 ± 5 (n = 3) peak pairs were detected by microflow LC-MS. Figure 4B shows that, for nanoLC-MS, the maximal number of peak pairs (2301 ± 86) was reached when 11.4 pmol of labeled lysate was injected.

Figure 4 shows that, at both optimal injection conditions, nanoLC-MS could detect 37% more metabolites than microflow LC-MS. It should be noted that the two QTOF instruments used gave almost the same detectability of labeled metabolites when microflow LC was linked to both. Thus, the detectability of nanoLC-MS is significantly better than microflow LC-MS. More importantly, for handling small amounts of samples, the sample amount needed to reach the maximal number of detectable peak pairs is about 200-fold less in nanoLC-MS than microflow LC-MS.

Metabolomic Profiling of Small Numbers of Cells. After optimizing sample handling and instrument settings, the CIL nanoLC-MS system was used to profile the amine/phenol

DOI: 10.1021/acs.analchem.7b03100
Anal. Chem. 2017, 89, 11664−11671

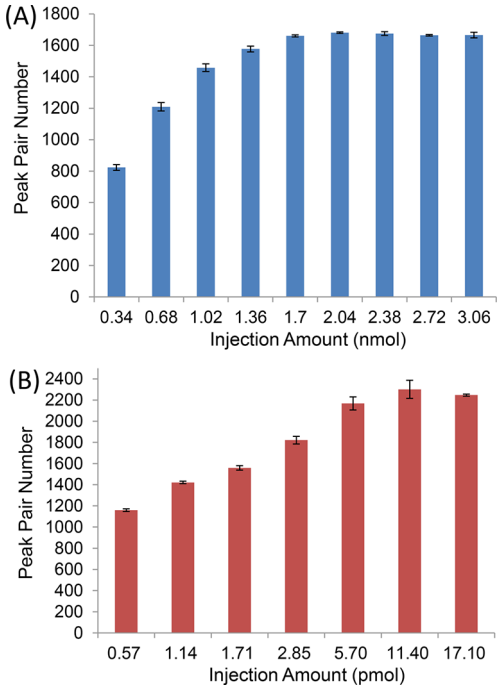

Figure 4. Average peak pair numbers detected using (A) microflow LC-MS and (B) nanoLC-MS as a function of injection amount of ^{12}C-/^{13}C-labeled cell lysates (n = 3).

submetabolome of 100, 1000, and 10000 cells. In each case, cells were lysed and then split into two aliquots with one aliquot for ^{12}C-labeling and another aliquot for ^{13}C-labeling, followed by mixing the labeled aliquots for nanoLC-MS analysis. Note that, in a metabolomics study of comparing different types of cells (e.g., wild type vs mutated cells), sample splitting of a cell lysate is needed in order to produce a pooled cell extract from mixing aliquots of all comparative cell lysates. This pooled sample is labeled with a ^{13}C-reagent to serve as a global internal control; an aliquot of ^{13}C-pool is spiked into a ^{12}C-labeled individual cell lysate for relative quantification. In some applications, we could replace the pooled sample with a cell lysate prepared from a large number of similar cells. If this could be done, we would not need to split a cell lysate and thus double the sample amount for LC-MS analysis (i.e., the current result of 100 cells would be equivalent to that from a starting material of 50 cells per sample).

For the labeled cell lysates prepared from 10000 cells, the amount of labeled metabolites was found to be ~120 pmol, which is higher than the optimal injection amount (i.e., 11.4 pmol). Thus, only the optimal amount was taken for injection into nanoLC-MS. However, the amount of labeled metabolites from 100 or 1000 cells could not be determined as it was below the detection limit of the current LC-UV setup; for future work, we plan to develop a fluorescence-based detection system for quantifying trace amounts of labeled metabolites. Nevertheless, the amount of labeled metabolites was expected to be less than the optimal injection amount and thus all the labeled lysates

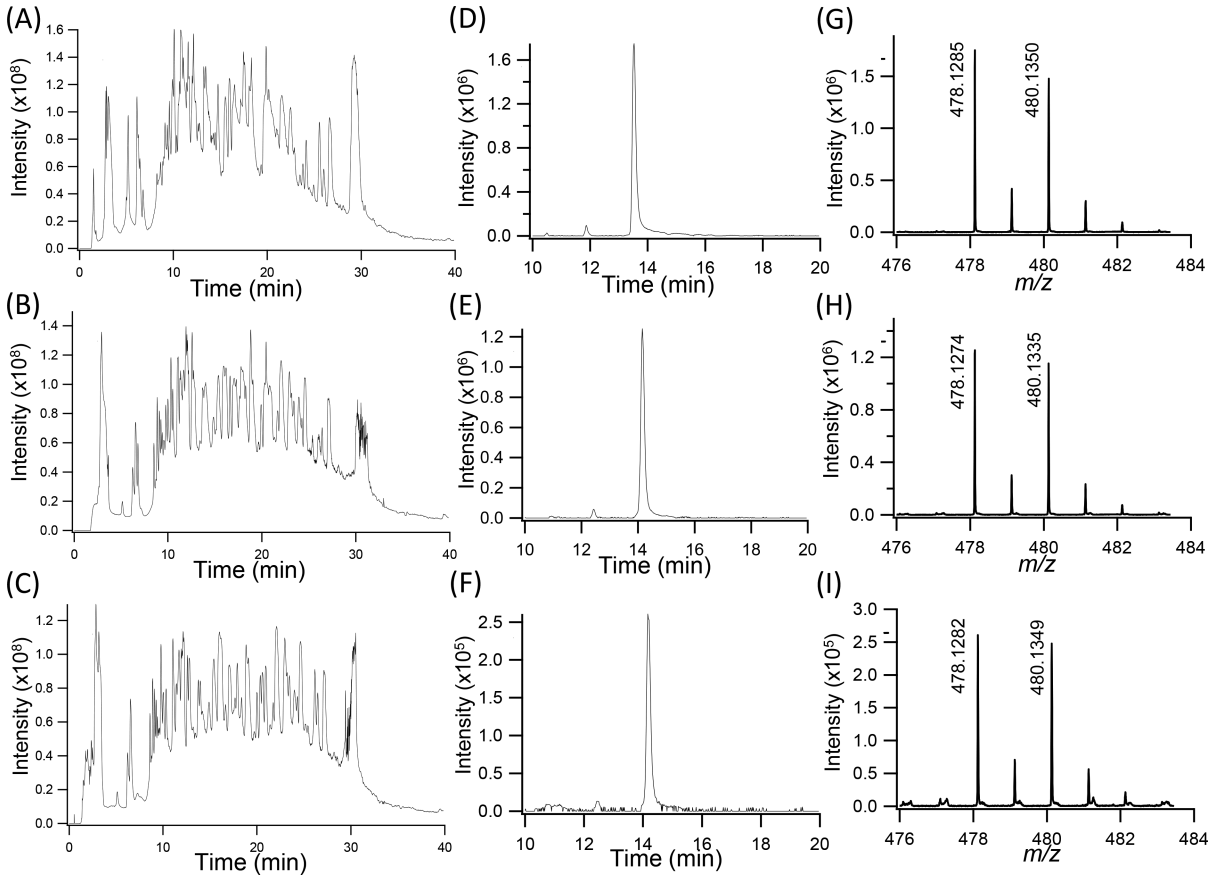

Figure 5. (A–C) Total ion chromatograms of labeled cell lysates, (D–F) extracted ion chromatograms of Dns-uridine, and (G–I) molecular ion regions of the ^{12}C-/^{13}C-Dns-uridine peak pair obtained from injection of 1/10 of the labeled 10000-cell lysate (top), all labeled 1000-cell lysate (middle), and all labeled 100-cell lysate (bottom).

DOI: 10.1021/acs.analchem.7b03100
Anal. Chem. 2017, 89, 11664–11671

from 100 or 1000 cells were injected. Figure 5A–C shows the representative total ion chromatograms generated from the labeled lysates of 100, 1000, and 10000 cells, while Figure 5D–F shows the corresponding extracted ion chromatograms (EIC) of a labeled metabolite (Dns-uridine) and Figure 5G–I shows the molecular ion regions of the detected peak pair. The signal-to-noise ratios of EICs and mass spectral peaks are slightly lower in the 1000-cell lysate, compared to the 1/10 injection of the 10000-cell lysate, suggesting that sample loss might be more severe in handling 1000 cells than working with 10000 cells. For the 100-cell lysate, the signal intensities are much lower than those from 1000 cells, as expected.

Figure 6 shows the plots of the number of peak pairs detected from these samples. There are 1620 ± 148, 2091 ± 89, and 2402 ± 80 (n = 6) peak pairs detected from the 100-, 1000-, and 10000-cell lysates, respectively. Comparing to 2402 peak pairs detected from the 10000-cell lysates, we were still able to detect ~87% peak pairs from 10-fold less cells, and ~67% peak pairs from 100-fold less cells. Figure 6B–D shows the Venn diagrams of peak pair numbers detected from experimental duplicate on biological triplicate analysis (n = 6). Most of peaks pairs could be detected from all the biological triplicate analysis (#1, #2, and #3), indicating excellent reproducibility of our workflow.

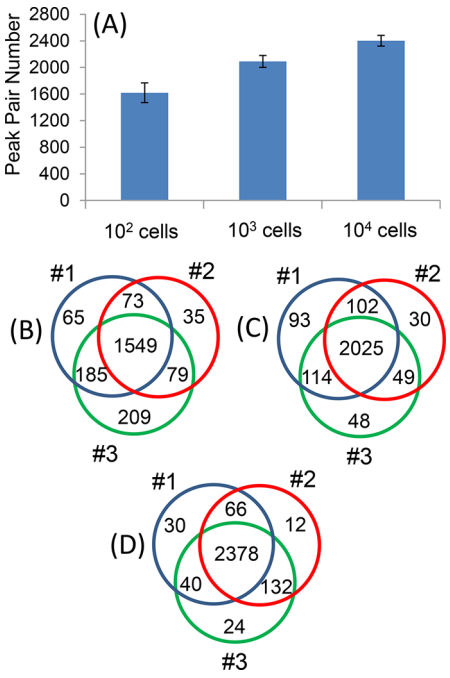

Figure 6. (A) Average peak pair numbers detected from ^{12}C-/^{13}C-labeled 100-, 1000-, and 10000-cell lysates (duplicate analysis of three biological replicates or n = 6). Venn diagrams of peak pair numbers detected from biological triplicate analysis of ^{12}C-/^{13}C-labeled cell lysates of (B) 100, (C) 1000, and (D) 10000 cells.

Many of the peak pairs detected could be identified or mass-matched to human metabolome databases. Using the dansyl standard library consisting of 278 amine/phenol-containing metabolites, we identified 80, 94, 106 metabolites from the 100-, 1000- and 10000-cell lysates, respectively (Supporting Information, Tables S2–S4). Based on accurate mass search with a mass tolerance of 10 ppm, we could match 673, 751, and 896 peak pairs to metabolite structures in HMDB (8021 entries; Supporting Information, Tables S5–S7) and additional 369, 474, and 511 peak pairs to the predicted metabolites in MCID (375,809 entries; Supporting Information, Tables S8–S10). In total, 1122 (69.3%), 1319 (63.1%), and 1513 (63.1%) peak pairs could be identified and matched in the 100-, 1000-, and 10000-cell lysates, respectively.

CONCLUSIONS

We have developed a CIL nanoLC-MS method for metabolomic profiling of small numbers of cells and demonstrated the metabolic coverage of this method for analyzing the amine/phenol submetabolome of 100, 1000, and 10000 MCF-7 breast cancer cells. To our knowledge, there is no other method reported in the literature that could match the performance of the described workflow in both quantification accuracy and coverage for analyzing 100 to 10000 mammalian cells. The potential impact of this work is that, when a bioscience researcher working on mammalian cells wishes to perform high-coverage quantitative metabolomics of 100 to 10000 cells, they now have the option of adapting the method described in this paper to do it.

Our research goal was to achieve the highest possible coverage in order to generate metabolome-wide metabolic information required for in-depth biological and biomarker discovery studies. In the case of 10000 cells, we have shown that only a fraction (10%) of the labeled lysate was needed to reach the optimal sample injection in nanoLC-MS for detecting the maximal number of peak pairs or metabolites. In future work, we will consider splitting a 10000-cell lysate into four aliquots to analyze, separately, the four submetabolomes (amines/phenols, carboxyls, hydroxyls, and carbonyls) to produce a very comprehensive profile of the cellular metabolome. We envisage that the CIL nanoLC-MS method can become a routine quantitative platform for cellular metabolomics with a starting material of 10000 cells. For analyzing 1000 or 100 cells, even with the injection of almost all the labeled samples, the coverage was found to be decreased to 2091 ± 89 pairs in the 1000-cell lysate and 1620 ± 148 pairs in the 100-cell lysate (n = 6), compared to 2402 ± 80 pairs found in the 10000-cell lysate. This level of coverage may find to be sufficient in some areas of applications such as partial mapping of the metabolic network or targeted analysis of detectable metabolites. However, future research in improving sample preparation, separation and MS detection including the use of miniaturized devices is needed to maximize the coverage in metabolomics of 1000, 100, or even a lower number of cells.

ASSOCIATED CONTENT

Supporting Information

The Supporting Information is available free of charge on the ACS Publications website at DOI: 10.1021/acs.analchem.7b03100.

Experimental details, Venn diagrams of solvent extractions, chromatograms of blank samples, physical properties of chemical vapors, and lists of metabolite identification results (PDF).

AUTHOR INFORMATION

Corresponding Author

*E-mail: liang.li@ualberta.ca.

ORCID

Liang Li: 0000-0002-9347-2108

DOI: 10.1021/acs.analchem.7b03100
Anal. Chem. 2017, 89, 11664–11671

Notes

The authors declare no competing financial interest.

■ ACKNOWLEDGMENTS

This work was supported by the Natural Sciences and Engineering Research Council of Canada, the Canada Research Chairs program, Genome Canada and Alberta Innovates.

■ REFERENCES

(1) Zamboni, N.; Saghatelian, A.; Patti, G. J. *Mol. Cell* **2015**, *58*, 699−706.
(2) Hounoum, B. M.; Blasco, H.; Emond, P.; Mavel, S. *TrAC, Trends Anal. Chem.* **2016**, *75*, 118−128.
(3) Shyh-Chang, N.; Ng, H. H. *Genes Dev.* **2017**, *31*, 336−346.
(4) Jackson, J. M.; Witek, M. A.; Kamande, J. W.; Soper, S. A. *Chem. Soc. Rev.* **2017**, *46*, 4245−4280.
(5) Datta, S.; Malhotra, L.; Dickerson, R.; Chaffee, S.; Sen, C. K.; Roy, S. *Histol. Histopath.* **2015**, *30*, 1255−1269.
(6) Comi, T. J.; Do, T. D.; Rubakhin, S. S.; Sweedler, J. V. *J. Am. Chem. Soc.* **2017**, *139*, 3920−3929.
(7) Zenobi, R. *Science* **2013**, *342*, 1243259.
(8) Amantonico, A.; Urban, P. L.; Zenobi, R. *Anal. Bioanal. Chem.* **2010**, *398*, 2493−2504.
(9) Li, L.; Golding, R. E.; Whittal, R. M. *J. Am. Chem. Soc.* **1996**, *118*, 11662−11663.
(10) Guillaume-Gentil, O.; Rey, T.; Kiefer, P.; Ibanez, A. J.; Steinhoff, R.; Bronnimann, R.; Dorwling-Carter, L.; Zambelli, T.; Zenobi, R.; Vorholt, J. A. *Anal. Chem.* **2017**, *89*, 5017−5023.
(11) Walker, B. N.; Antonakos, C.; Retterer, S. T.; Vertes, A. *Angew. Chem., Int. Ed.* **2013**, *52*, 3650−3653.
(12) Shrestha, B.; Vertes, A. *Anal. Chem.* **2009**, *81*, 8265−8271.
(13) Fujii, T.; Matsuda, S.; Tejedor, M. L.; Esaki, T.; Sakane, I.; Mizuno, H.; Tsuyama, N.; Masujima, T. *Nat. Protoc.* **2015**, *10*, 1445−1456.
(14) Gong, X. Y.; Zhao, Y. Y.; Cai, S. Q.; Fu, S. J.; Yang, C. D.; Zhang, S. C.; Zhang, X. R. *Anal. Chem.* **2014**, *86*, 3809−3816.
(15) Yang, W. C.; Regnier, F. E.; Jiang, Q.; Adamec, J. *J. Chromatogr. A* **2010**, *1217*, 667−675.
(16) Dai, W. D.; Huang, Q.; Yin, P. Y.; Li, J.; Zhou, J.; Kong, H. W.; Zhao, C. X.; Lu, X.; Xu, G. W. *Anal. Chem.* **2012**, *84*, 10245−10251.
(17) Leng, J. P.; Wang, H. Y.; Zhang, L.; Zhang, J.; Wang, H.; Guo, Y. L. *Anal. Chim. Acta* **2013**, *758*, 114−121.
(18) Tayyari, F.; Gowda, G. A. N.; Gu, H. W.; Raftery, D. *Anal. Chem.* **2013**, *85*, 8715−8721.
(19) Yuan, W.; Li, S. W.; Edwards, J. L. *Anal. Chem.* **2015**, *87*, 7660−7666.
(20) Mochizuki, T.; Todoroki, K.; Inoue, K.; Min, J. Z.; Toyo'oka, T. *Anal. Chim. Acta* **2014**, *811*, 51−59.
(21) Chu, J. M.; Qi, C. B.; Huang, Y. Q.; Jiang, H. P.; Hao, Y. H.; Yuan, B. F.; Feng, Y. Q. *Anal. Chem.* **2015**, *87*, 7364−7372.
(22) Arrivault, S.; Guenther, M.; Fry, S. C.; Fuenfgeld, M.; Veyel, D.; Mettler-Altmann, T.; Stitt, M.; Lunn, J. E. *Anal. Chem.* **2015**, *87*, 6896−6904.
(23) Wong, J. M. T.; Malec, P. A.; Mabrouk, O. S.; Ro, J.; Dus, M.; Kennedy, R. T. *J. Chromatogr. A* **2016**, *1446*, 78−90.
(24) Yu, L.; Ding, J.; Wang, Y. L.; Liu, P.; Feng, Y. Q. *Anal. Chem.* **2016**, *88*, 1286−1293.
(25) Hao, L.; Johnson, J.; Lietz, C. B.; Buchberger, A.; Frost, D.; Kao, W. J.; Li, L. J. *Anal. Chem.* **2017**, *89*, 1138−1146.
(26) Guo, K.; Li, L. *Anal. Chem.* **2009**, *81*, 3919−3932.
(27) Guo, K.; Li, L. *Anal. Chem.* **2010**, *82*, 8789−8793.
(28) Zhao, S.; Luo, X.; Li, L. *Anal. Chem.* **2016**, *88*, 10617−10623.
(29) Zhao, S.; Dawe, M.; Guo, K.; Li, L. *Anal. Chem.* **2017**, *89*, 6758−6765.
(30) Luo, X.; Zhao, S.; Huan, T.; Sun, D.; Friis, R. M. N.; Schultz, M. C.; Li, L. *J. Proteome Res.* **2016**, *15*, 1602−1612.
(31) Wu, Y. M.; Li, L. *Anal. Chem.* **2012**, *84*, 10723−10731.
(32) Zhou, R.; Tseng, C. L.; Huan, T.; Li, L. *Anal. Chem.* **2014**, *86*, 4675−4679.
(33) Huan, T.; Li, L. *Anal. Chem.* **2015**, *87*, 7011−7016.
(34) Huan, T.; Li, L. *Anal. Chem.* **2015**, *87*, 1306−1313.
(35) Huan, T.; Wu, Y. M.; Tang, C. Q.; Lin, G. H.; Li, L. *Anal. Chem.* **2015**, *87*, 9838−9845.
(36) Li, L.; Li, R. H.; Zhou, J. J.; Zuniga, A.; Stanislaus, A. E.; Wu, Y. M.; Huan, T.; Zheng, J. M.; Shi, Y.; Wishart, D. S.; Lin, G. H. *Anal. Chem.* **2013**, *85*, 3401−3408.
(37) Wang, N.; Xu, M.; Wang, P.; Li, L. *Anal. Chem.* **2010**, *82*, 2262−2271.
(38) Brown, R. B.; Audet, J. *J. R. Soc., Interface* **2008**, *5*, S131−S138.
(39) Wu, Y. M.; Li, L. *Anal. Chem.* **2013**, *85*, 5755−5763.
(40) Uehara, T.; Yokoi, A.; Aoshima, K.; Tanaka, S.; Kadowaki, T.; Tanaka, M.; Oda, Y. *Anal. Chem.* **2009**, *81*, 3836−3842.
(41) Yuan, W.; Anderson, K. W.; Li, S. W.; Edwards, J. L. *Anal. Chem.* **2012**, *84*, 2892−2899.
(42) Jones, D. R.; Wu, Z. P.; Chauhan, D.; Anderson, K. C.; Peng, J. M. *Anal. Chem.* **2014**, *86*, 3667−3675.
(43) Chetwynd, A. J.; Abdul-Sada, A.; Hill, E. M. *Anal. Chem.* **2015**, *87*, 1158−1165.
(44) Li, Z. D.; Tatlay, J.; Li, L. *Anal. Chem.* **2015**, *87*, 11468−11474.
(45) Li, Z. D.; Li, L. *Anal. Chem.* **2014**, *86*, 331−335.

DOI: 10.1021/acs.analchem.7b03100
Anal. Chem. 2017, 89, 11664−11671